

Supporting Information

**Selective Activation of C–H Bonds in a Cascade Process Combining
Photochemistry and Biocatalysis**

*Wuyuan Zhang⁺, Bastien O. Burek⁺, Elena Fernández-Fueyo, Miguel Alcalde,
Jonathan Z. Bloh,^{*} and Frank Hollmann^{*}*

anie_201708668_sm_miscellaneous_information.pdf

Supporting Information

Table of Contents

Table of Contents	2
Experimental procedures	3
__ Preparation of the photocatalyst.....	3
__ Enzyme preparation.....	3
__ Protein purification	3
__ Photochemical setup.....	4
__ Photocatalytic steady-state hydrogen peroxide generation.....	5
__ Quantitative OH-Radical detection using the coumarin hydroxylation method	5
__ Actinometry.....	5
__ Characterization of Au-TiO ₂	6
__ Preparative-scale photoenzymatic synthesis.....	7
Analytical procedures	8
__ Details on the GC analytics and representative chromatograms	8
Further experimental results	13
__ Control experiments to validate the reaction scheme	13
__ Evaporation experiments: effect of exposing the reaction mixture to the ambient atmosphere.	13
__ Influence of the methanol concentration on the photoenzymatic hydroxylation of ethyl benzene.	14
__ Influence of the methanol concentration on the steady-state H ₂ O ₂ concentration.	14
__ Influence of the photocatalyst concentration on the photoenzymatic hydroxylation of ethyl benzene.	15
__ Influence of the photocatalyst concentration on the steady-state H ₂ O ₂ concentration.	15
__ Influence of the biocatalyst concentration on the photoenzymatic hydroxylation of ethyl benzene.	16
__ Use of different sacrificial electron donors for the photochemoenzymatic hydroxylation of ethyl benzene.	17
__ Influence of different sacrificial electron donors on the steady-state H ₂ O ₂ concentration.	17
__ Influence of formaldehyde or formic acid as sacrificial electron donors on the photochemoenzymatic hydroxylation of ethyl benzene.	18
__ Influence of formaldehyde or formic acid as sacrificial electron donors on the steady-state H ₂ O ₂ concentration using rutile Au-TiO ₂	18
__ Influence of the photocatalyst loading on the optical transparency of the reaction mixture	19
__ NRM-spectroscopic analysis of the Au-TiO ₂ -catalysed oxidation of methanol.	19
__ NRM-spectroscopic analysis of the Au-TiO ₂ -catalysed oxidation of formaldehyde.....	20
__ Comparison of photoenzymatic reactions in the presence and absence of methanol as sacrificial electron donor	21
__ Effect of methanol on the stability of rAaeUPO in the presence of Au-TiO ₂	22
__ Influence of Methanol on the formation rate of hydroxyl radicals	22
Additional information	23
__ Elementary steps in Au-TiO ₂ -catalysed oxidation of water and methanol.	23
__ Overview over literature-reported hydroxylation reactions and <i>in situ</i> H ₂ O ₂ generation systems.	24
Contributions	25
References	26

Experimental procedures

Chemicals: Unless indicated otherwise all chemicals were purchased from Sigma-Aldrich, Fluka, Acros or Alfa-Aesar in the highest purity available and used without further treatment. Titanium (IV) oxide (TiO₂, anatase) was bought from Sigma-Aldrich (The Netherlands) and used as received. Rutile TiO₂ was synthesized via a gas phase deposition method (confirmed by the supplier). Anatase TiO₂ used here consisted of rutile and anatase (9 : 91). Gold(III) chloride (64.4% minimum) was brought from Alfa-Aesar.

Preparation of the photocatalyst

The preparation of Au-TiO₂ was based on a previously reported method:^[1] To deposit Au nanoparticles onto the surface of TiO₂, the so-called deposition-precipitation method was used: an aqueous solution of AuCl₃ (5 mM, slight yellow) was heated to 70 °C and the pH adjusted with 0.1 M NaOH to 7.2. 11 mL of this solution were added to 97 mL MilliQ water (pre-heated to 70 °C). After stirring for 10 minutes 1g of TiO₂ particles were added and the suspension was stirred for 1 hour at 70 °C. After cooling to room temperature, the mixture was stirred for another 1 hour. The resulting Au-TiO₂ nanoparticles were centrifuged (6000 rpm for 15 min), washed three times with MillQ water and dried at 70 °C overnight.

Enzyme preparation

The recombinant unspecific peroxygenase from *Agrocybe aegerita* (rAaeUPO) evolved for functional expression in yeast^[2] was produced and purified as described previously.^[3] The *P. pastoris* culture broth containing rAaeUPO was clarified by centrifugation at 8000 rpm for 2 hours at 4 °C. The supernatant was filtered through a 20 µm filter and stored at -80 °C. The activity of rAaeUPO was determined to be 652 ± 5 U mg⁻¹ (pH 5.0 in NaPi buffer) after purification. One unit of the enzyme activity was defined as the amount of the enzyme catalysing the oxidation of 1 µmol of ABTS per minute.

Protein purification

The supernatant was concentrated (Amicon 10-kDa-cut-off) and dialysed against 100 mM sodium phosphate, pH 7. rAaeUPO was purified using a NGC Chromatography system (Biorad) in one single step. The separation was performed on a Q Sepharose FF 30-mL cartridge with a flow rate of 5 mL min⁻¹. After 90 mL, the retained protein was eluted with a 0-50 % NaCl gradient in 450 mL, followed by 50-100 % gradient in 50 mL and 100 % NaCl in 75 mL. Peroxygenase activity was followed by ABTS oxidation in the presence of H₂O₂, and the appropriate fractions were pooled, concentrated and dialysed against 100 mM sodium phosphate buffer (pH 7).

The UV/Vis spectrum of purified rAaeUPO showed a Reinheitszahl (Rz: A420/A280) value of 1.6 and was essentially pure as judged by SDS-PAGE (Figure S1).

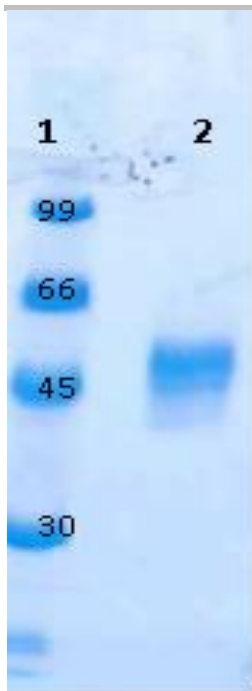


Figure S1. SDS-PAGE gel (12 % stained with Coomassie brilliant blue R-250) of the purified rAaeUPO. Lane 1 standard (99 kDa, 66 kDa, 45 kDa and 30 kDa) and lane 2 purified enzyme.

The concentration of rAaeUPO was determined using the molar extinction coefficient of $115 \text{ mM}^{-1} \text{ cm}^{-1}$ at 420 nm. Absorption spectrum in the UV/Vis range was recorded in a Biomate5 (Thermo) spectrophotometer.

Photochemical setup

Photoenzymatic reactions were performed at 30 °C in 1.0 mL of sodium phosphate buffer (60 mM NaPi, pH 7.0). Unless mentioned otherwise, 5.0 mg of the photocatalyst (Au-TiO_2) were suspended in 900 μL of the buffer (5 min in an ultrasonication bath), afterwards aliquots of rAaeAPO (150 nM final), methanol (250 mM final) and substrates (15 mM final) were added. The reaction vial was closed, and exposed to visible light bulb (Philips 7748XHP 205W, white light bulb) under gentle stirring (Figure S2). The distance between the reaction vial and bulb was 3.6 cm. At intervals, aliquots were withdrawn, extracted with ethyl acetate (containing 5 mM of 1-octanol/dodecane as internal standard) and analysed by Gas Chromatography (*vide infra*).



Figure S2. Image of homemade photocatalytic setup.

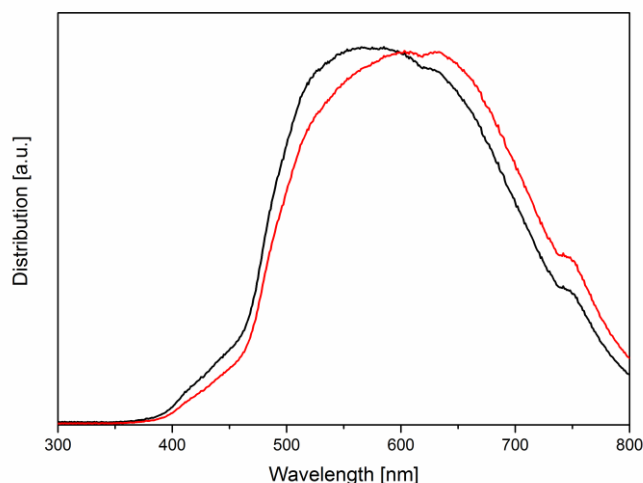


Figure S3. The radiant flux distribution (black line) of the lamp. The measurement used an Ocean Optics FLAME-S-UV-VIS-ES fibre optic spectrophotometer and the calculated photon flux distribution (red line).

Photocatalytic steady-state hydrogen peroxide generation

Photocatalytic steady-state hydrogen peroxide generation using Au-TiO₂ was performed at 30 °C in 1.0 mL of sodium phosphate buffer (60 mM NaPi, pH 7.0). Unless mentioned otherwise, 5.0 mg of photocatalyst and 250 mM of methanol were used. The reaction vial was closed, and exposed to the light source (Philips 7748XHP 205 W, white light bulb) under gentle stirring. To analyse the concentration of H₂O₂, the fluorometric method by Guilbault was used:^[4] Horse radish peroxidase (HRP) catalyzed, H₂O₂-dependent dimerisation of *p*-hydroxyphenylacetic acid (POHPAA) yielded the fluorescent product. Specifically, lyophilised powder of HRP (1 mg, 163 U mg⁻¹, Type II, Sigma) was dissolved in TRIS buffer (12.5 mL, pH 8.8, 1 M, Alfa Aesar). POHPAA (4 mg, Alfa Aesar, recrystallized twice from water) was dissolved in TRIS buffer (12.5 mL). 12.5 μL of each solution were added to 100 μL sample solution (filtered through a PVDF syringe filter (0.2 μm, Roth) to remove the TiO₂ particles). The fluorescence signal (λ_{ex} = 315 nm, λ_{em} = 406 nm, 25°C) was determined in a microplate reader (SynergyMx, BioTek). The concentration-time profiles of peroxide formation were analysed using the kinetic model developed by Kormann et al., see eq. 1.^[5] Non-linear regression (Levenberg-Marquardt algorithm) of the experimental data to the model yields the kinetic parameters formation rate *k_F* and degradation rate *k_D*.

$$c = \frac{k_F}{k_D} + e^{-k_D t} \left(c_0 - \frac{k_F}{k_D} \right) \quad (1)$$

Quantitative OH-Radical detection using the coumarin hydroxylation method

Coumarin hydroxylation reactions using Au-TiO₂ were performed at 30 °C in 1.0 mL of sodium phosphate buffer (60 mM NaPi, pH 7.0). 0.1 mM coumarin (Aldrich), 5.0 mg of photocatalyst and 250 mM of methanol were used. The reaction vial was closed and irradiated under gentle stirring. To analyse the concentration of umbelliferone, samples were taken and TiO₂ was separated via centrifugation. The fluorescence signal (λ_{ex} = 332 nm, λ_{em} = 455 nm, 25°C) of 100 μL of the supernatant was measured in a microplate reader. The amount of OH-radicals was calculated assuming 6.1 % of coumarin being hydroxylated to umbelliferone.^[6]

Actinometry

Chemical actinometry was performed at 30 °C in 1.0 mL of 150 mM potassium ferrioxalate solution (freshly prepared by mixing potassium oxalate and iron(III) chloride and recrystallized from water) in 50 mM sulfuric acid. The reaction vial was closed and irradiated under gentle stirring in a darkened room to avoid interference from other light sources. The amount of Fe(II) formed was determined via the absorbance of the ferrioxalate complex: 25 μL of samples were diluted with 20 μL of 0.1% aqueous 1,10-phenanthroline solution, 75 μL of 50 mM sulfuric acid, 50 μL of 1 M acetate buffer. The final volume of the mixture was adjusted to 200 μL with MilliQ water. The absorbance at 510 nm was measured in a microplate reader.

The photon flux density φ was calculated by integrating over the whole wavelength range, see eq. 2, where $\phi(\lambda)$ is the wavelength-dependent quantum yield of the photochemical ferrioxalate-reduction to Fe(II) obtained via linear interpolation of the values given in

Ref ^[7], $T(\lambda)$ is the transmission spectrum of the ferrioxalate solution in the reaction vessel, and lamp $I(\lambda)$ is the photon flux distribution of the lamp. The resulting photon flux density is $792 \mu\text{E L}^{-1} \text{ s}^{-1}$ which amounts to a radiant flux density of 157 W L^{-1} .

$$\varphi = \int \phi(\lambda) \cdot I(\lambda) \cdot (1 - T(\lambda)) d\lambda \quad (2)$$

Characterization of Au-TiO₂

The structures of the photocatalysts were characterized by a Bruker D8 Advance X-ray diffractometer using Co-K α radiation ($\lambda = 1.789 \text{ \AA}$) at 35 kV and 40 mA. The data were collected from $2\theta = 5.0^\circ - 80^\circ$ with a step size of 0.020° and a counting time of 0.5 s per step. The particle size and morphology were analysed by using Philips CM30TEM.

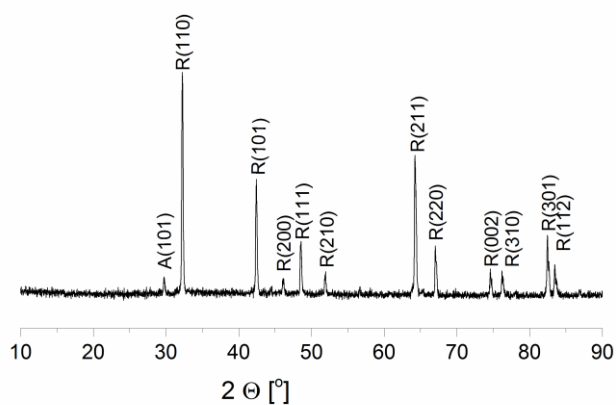


Figure S4. XRD pattern of the Au-TiO₂ photocatalyst.

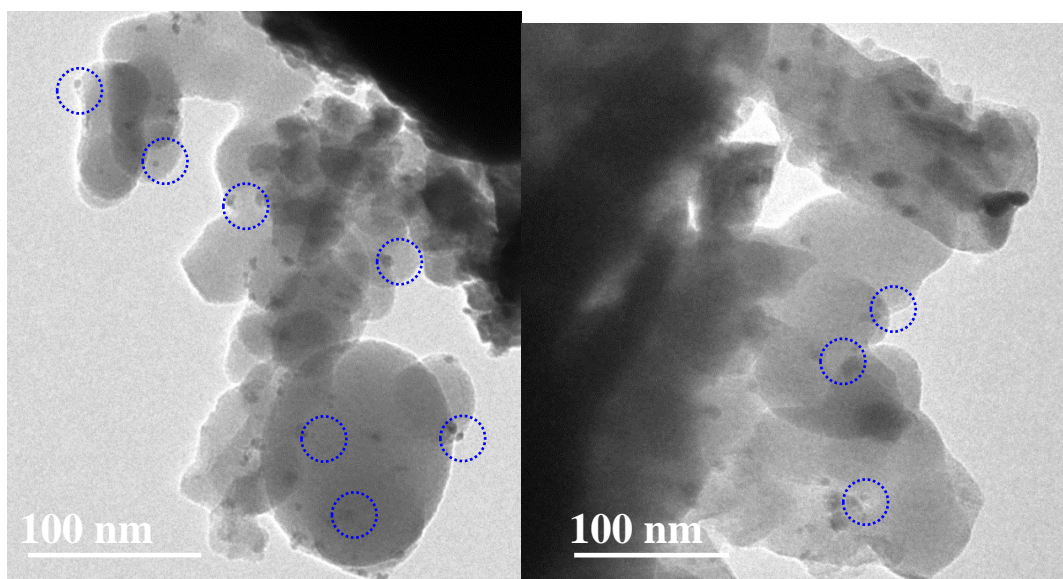


Figure S5. TEM images of the Au-TiO₂ photocatalyst.

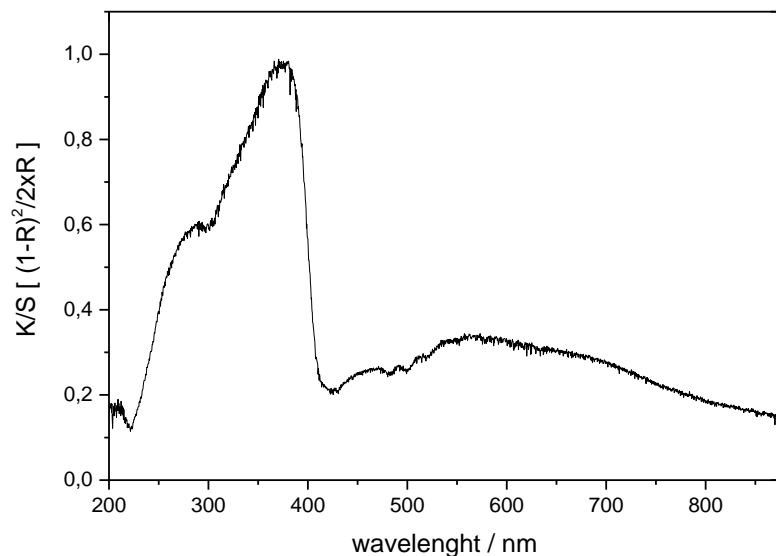


Figure S6. Apparent absorption spectrum of the Au-TiO₂ catalyst. The absorption was calculated from the diffuse reflectance spectrum (against BaSO₄ as total reflection standard) using the Kubelka-Munk transform.^[8]

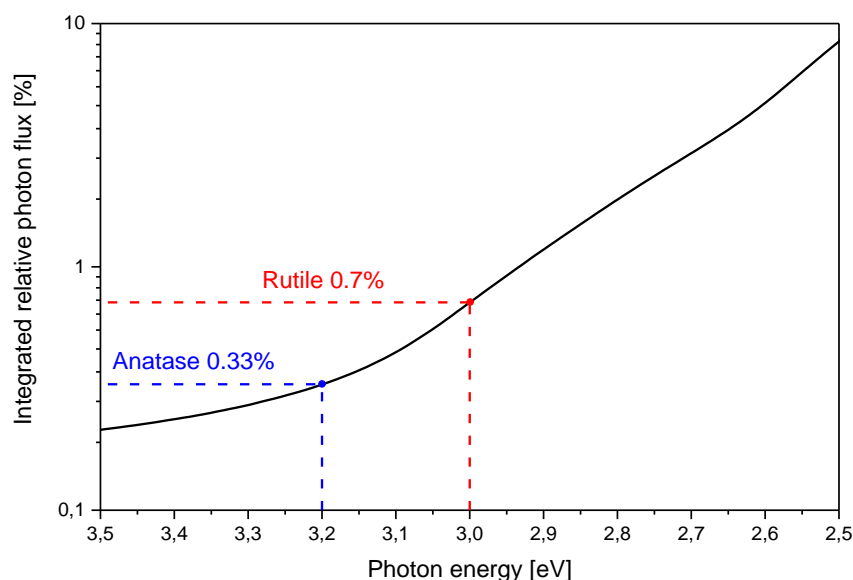


Figure S7. The integrated relative photon flux of the lamp spectrum plotted against the photon energy, *i.e.*, which fraction of the photon flux can be used by a material with a specific band gap. Displayed are the values for anatase and rutile TiO₂ with 3.2 eV and 3.0 eV band gap, respectively.

Preparative-scale photoenzymatic synthesis

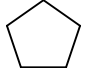

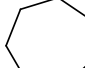
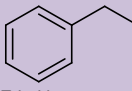
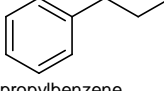
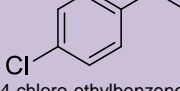
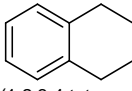

The preparative-scale synthesis of (*R*)-1-phenylethanol was carried out as follows: to a 250 mL glass bottle, 10 mg mL⁻¹ of rutile Au-TiO₂, 200 nM of rAaeUPO, 250 mM of methanol and 20 mM of ethyl benzene (final concentrations each) were added into sodium phosphate buffer (60 mM NaPi, pH 7.0). The reaction volume was adjusted to 100 mL using the same buffer. The mixture was irradiated for 93 hours under visible light at 30 °C after which it contained 12.26 mM (*R*)-1-phenylethanol, 1.34 mM acetophenone and 4.47 mM ethyl benzene (determined via GC).

The reaction mixture was centrifuged and the supernatant extracted with 50 mL of DCM (3×), dried over anhydrous MgSO₄ and purified with flash column chromatography (petroleum ether : ethyl acetate = 9.5 : 0.5). Overall, 0.1074 g of (*R*)-1-phenylethanol (97 % ee) was obtained (51 % isolated yield).

Analytical procedures

Details on the GC analytics and representative chromatograms

Table S1. Details of GC analysis.

Substrate	Analysis, column ^[a]	T _R [min] ^[b]	Temperature profile
 cyclopentane	Column A	cyclopentanol 7.83 cyclopentanone 6.33 IS 11.68	90 °C hold 3 min, 10 °C /min to 180 °C hold 1 min, 30 °C /min to 230 °C hold 1 min.
 cyclohexane	Column A	cyclohexanol 9.57 cyclohexanone 8.24 IS 11.68	90 °C hold 3 min, 10 °C /min to 180 °C hold 1 min, 30 °C /min to 230 °C hold 1 min.
 cycloheptane	Column A	cycloheptanol 12.08 cycloheptanone 10.47 IS 11.68	90 °C hold 3 min, 10 °C /min to 180 °C hold 1 min, 30 °C /min to 230 °C hold 1 min.
 Ethyl benzene	Quantification: Column A Enantiomeric excess: Column B	Quantification: ethylbenzene 2.95 1-phenylethanol 9.06 acetophenone 7.55 Enantiomeric excess: (<i>R</i>)-1-phenylethanol 14.96 (<i>S</i>)-1-phenylethanol 15.95	Quantification: 130 °C hold 3 min, 30 °C /min to 200 °C hold 4.5 min, 30 °C /min to 250 °C hold 1.5 min. Enantiomeric excess: 100 °C hold 4 min, 10 °C /min to 120 °C hold 10 min, 25 °C /min to 215 °C hold 1.3 min. Split ratio 50.
 propylbenzene	Quantification: Column A Enantiomeric excess: Column B	Quantification: propylbenzene 3.97 1-Phenyl-1-propanol 12.26 1-phenylpropanone 10.21 IS 7.07 Enantiomeric excess: (<i>R</i>)-1-Phenyl-1-propanol 12.05 (<i>S</i>)-1-Phenyl-1-propanol 12.33	Quantification: 120 °C hold 2 min, 15 °C /min to 180 °C hold 3 min, 30 °C /min to 200 hold 3 min, 30 °C /min to 245 hold 1 min. Enantiomeric excess: 120 °C hold 3 min, 5 °C /min to 135 °C hold 8 min, 25 °C /min to 210 °C hold 1 min. Split ratio 40.
 4-chloro-ethylbenzene	Quantification: Column A Enantiomeric excess: Column B	Quantification: 4-chloro-ethylbenzene 4.08 4-chloro-1-phenylethanol 10.17 4-Cl-acetophenone 13.81 IS 4.81 Enantiomeric excess: (<i>R</i>)-4-chloro-1-phenylethanol 12.47 (<i>S</i>)-4-chloro-1-phenylethanol 12.91	Quantification: 150 °C hold 1.5 min, 30 °C /min to 180 °C hold 4 min, 30 °C /min to 210 °C hold 3 min, 30 °C /min to 225 °C hold 3.5 min, 30 °C /min to 245 °C hold 1.5 min. Enantiomeric excess: 120 °C hold 3 min, 10 °C /min to 150 °C hold 4 min, 10 °C /min to 165 °C hold 3.5 min, 25 °C /min to 210 °C hold 2 min. Split ratio 40.
 (1,2,3,4-tetranaphthalene)	Quantification: Column A Enantiomeric excess: Column B	Quantification: 1,2,3,4-tetranaphthalene 7.14 α -Tetralol 16.15 α -Tetralone 14.65 IS 6.70 Enantiomeric excess: (<i>R</i>)- α -tetralol 23.95 (<i>S</i>)- α -tetralol 23.38	Quantification: 130 °C hold 3 min, 15 °C /min to 180 °C hold 1.3 min, 15 °C /min to 225 °C hold 6 min, 30 °C /min to 245 °C hold 1 min. Enantiomeric excess: 120 °C hold 3 min, 5 °C /min to 140 °C hold 19 min, 25 °C /min to 210 °C hold 2.5 min. Split ratio 40.
 octane	Quantification: Column A Enantiomeric excess: ^[d] Column B	Quantification: 2-octanol 4.96 1-octanol 6.65 IS 3.13 ^[c] Enantiomeric excess: ^[d] (<i>R</i>)-2-octanol 8.87 (<i>S</i>)-2-octanol 7.97	Quantification: 130 °C hold 3 min, 30 °C /min to 170 °C hold 2.7 min, 30 °C /min to 240 °C hold 1.2 min. Enantiomeric excess: 100 °C hold 4 min, 10 °C /min to 120 °C hold 3.2 min, 25 °C /min to 215 °C hold 2 min. Split ratio 50.

^[a] Column A: CP Wax 52 CB column (25 m × 0.25 mm × 1.2 μ m), FID, N₂ is the carrier gas; Column B: Chirasil Dex CB column (25 m × 0.32 mm × 0.25 μ m), FID, He is the carrier gas; Column C: Cpsil 5 CB: (50 m × 0.53 mm × 1.0 μ m), FID, N₂ is the carrier gas. ^[b] 1-Octanol (5 mM in ethyl acetate) is used as internal standard (IS) except otherwise note. ^[c] dodecane (5 mM in ethyl acetate) is used as IS. ^[d] In order to measure the ee, 3 mg of *N,N*-Dimethylpyridin-4-amine (DMAP) and 10 μ L of acetic anhydride were added to the ethyl acetate containing the 2-octanol (after extracting and drying the samples). The mixture was kept at 30 °C for 45 minutes, then 100 μ L of MilliQ water was added to stop the acetylation. The organic phase was dried over MgSO₂ and measured.

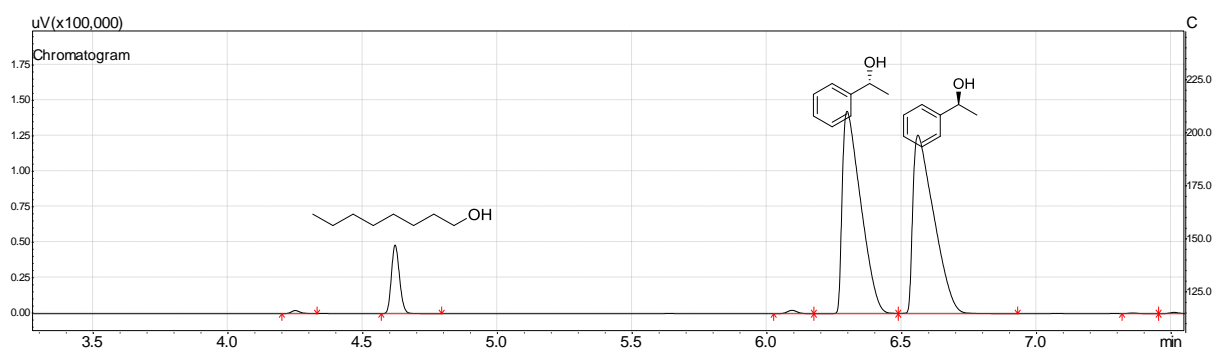


Figure S8. Representative GC chromatogram of racemic 1-phenyl ethanol.

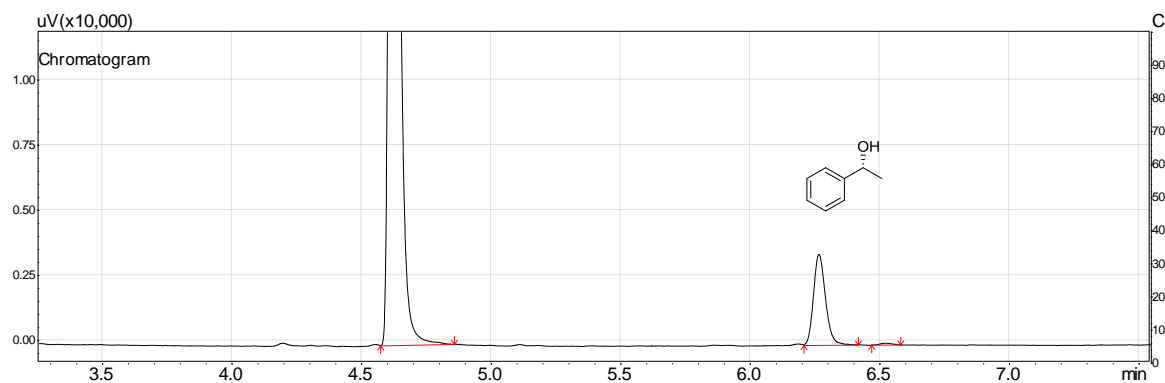


Figure S9. Representative GC chromatogram of the *rAaeJPO*-catalysed oxyfunctionalization of ethyl benzene to (*R*)-1-phenyl ethanol driven by rutile Au-TiO₂ catalysed methanol oxidation.

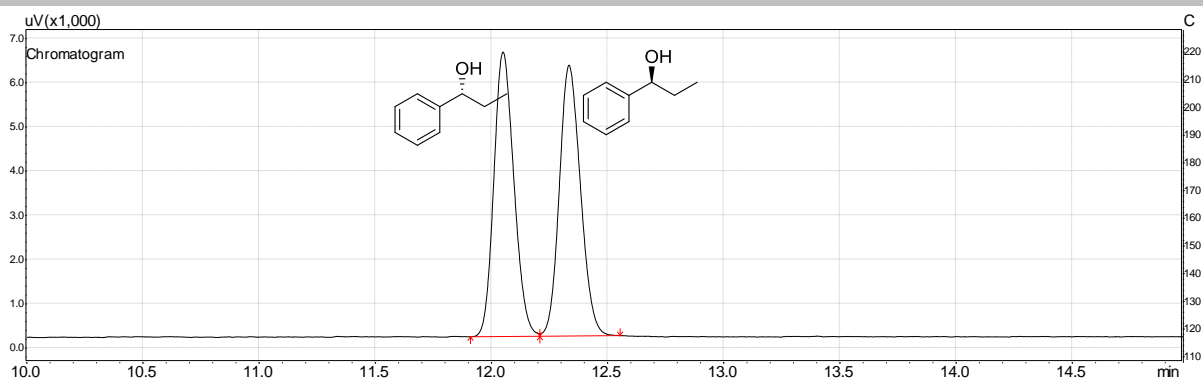


Figure S10. Representative GC chromatogram of racemic 1-phenyl-1-propanol.

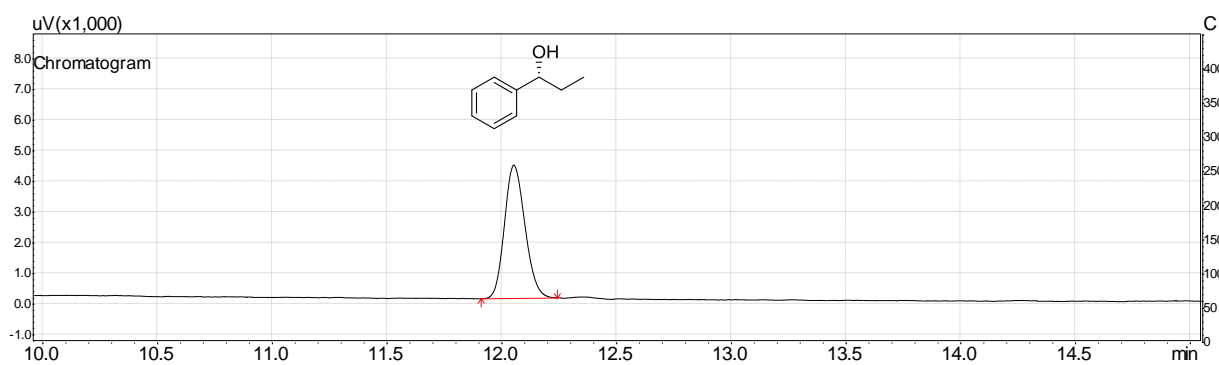


Figure S11. Representative GC chromatogram of the rAaeUPO-catalysed oxyfunctionalization of propylbenzene to (*R*)-1-phenyl-1-propanol driven by rutile Au-TiO₂ catalysed methanol oxidation.

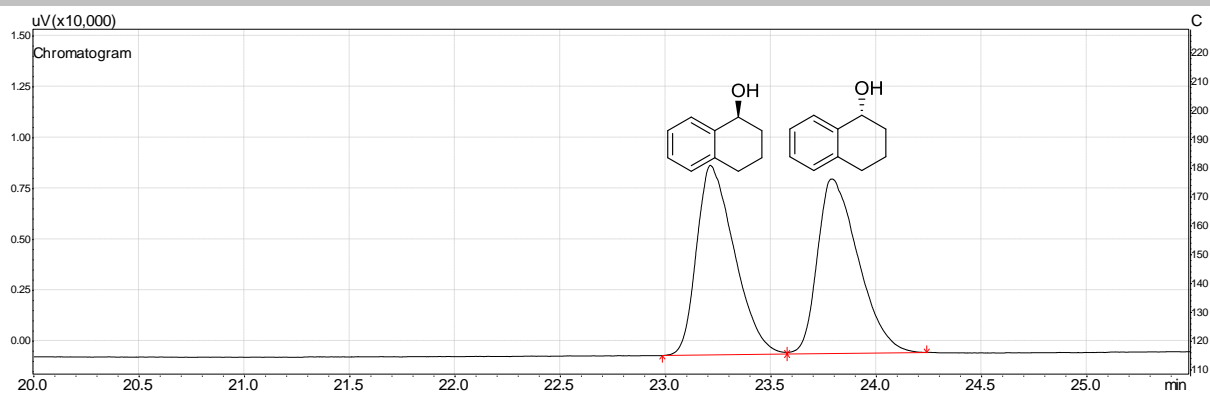


Figure S12. Representative GC chromatogram of racemic 1,2,3,4-tetrahydro-1-naphthol.

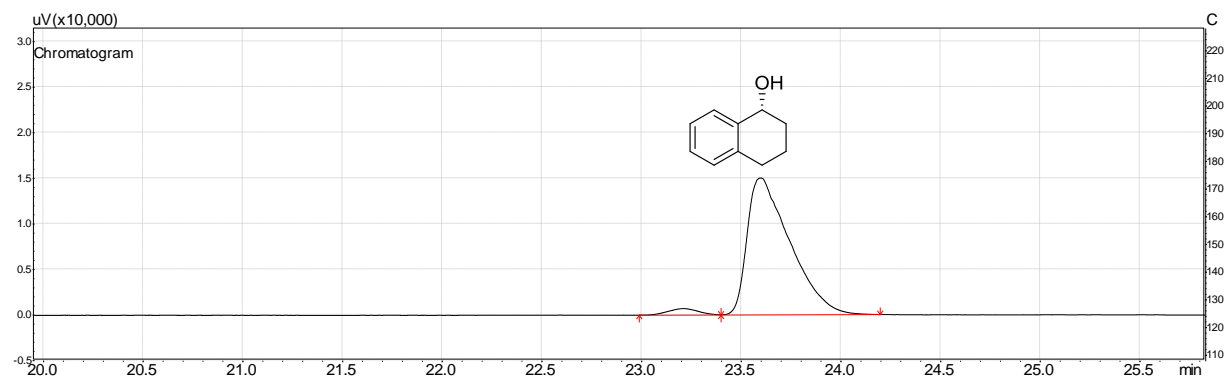


Figure S13. Representative GC chromatogram of the rAaeUPO-catalysed oxyfunctionalization of 1,2,3,4-tetrahydro-1-naphthol driven by rutile Au-TiO₂ catalysed methanol oxidation.

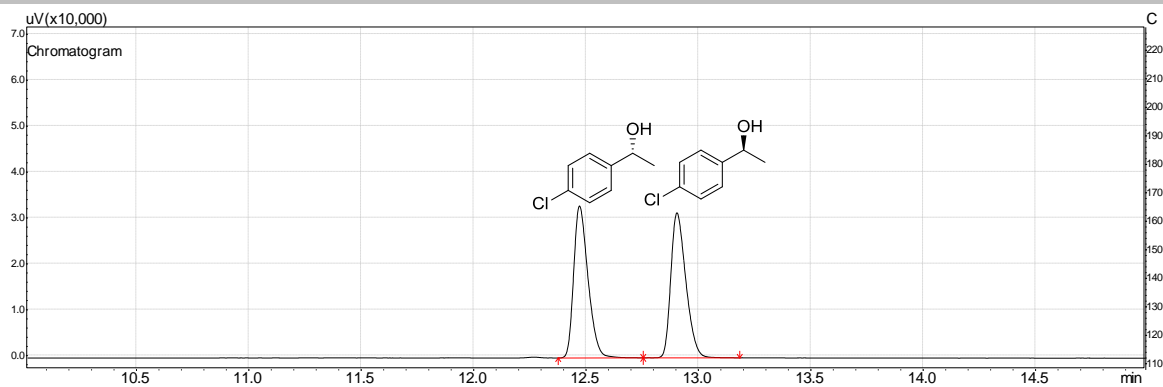


Figure S14. Representative GC chromatogram of racemic 4-chloro-1-phenylethanol.

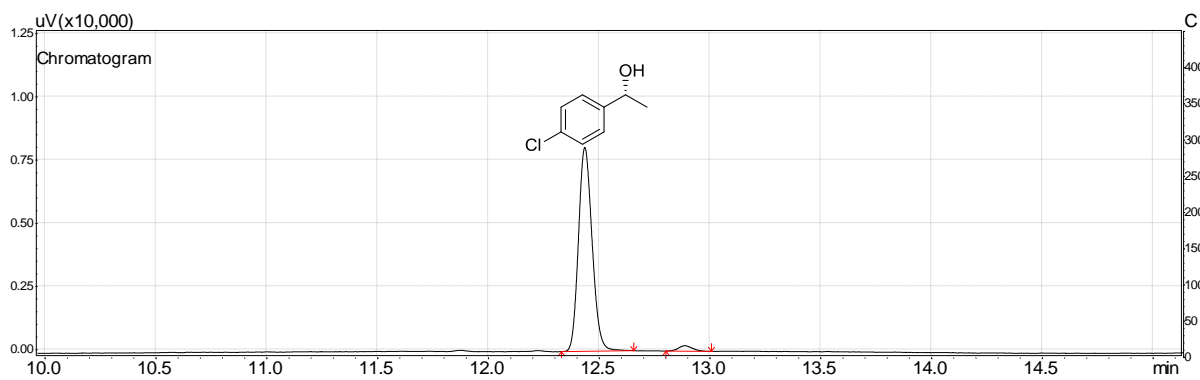


Figure S15. Representative GC chromatogram of the rAaeUPO-catalysed oxyfunctionalization of 4-chloro-ethyl benzene driven by rutile Au-TiO₂ catalysed methanol oxidation.

Further experimental results

Control experiments to validate the reaction scheme.

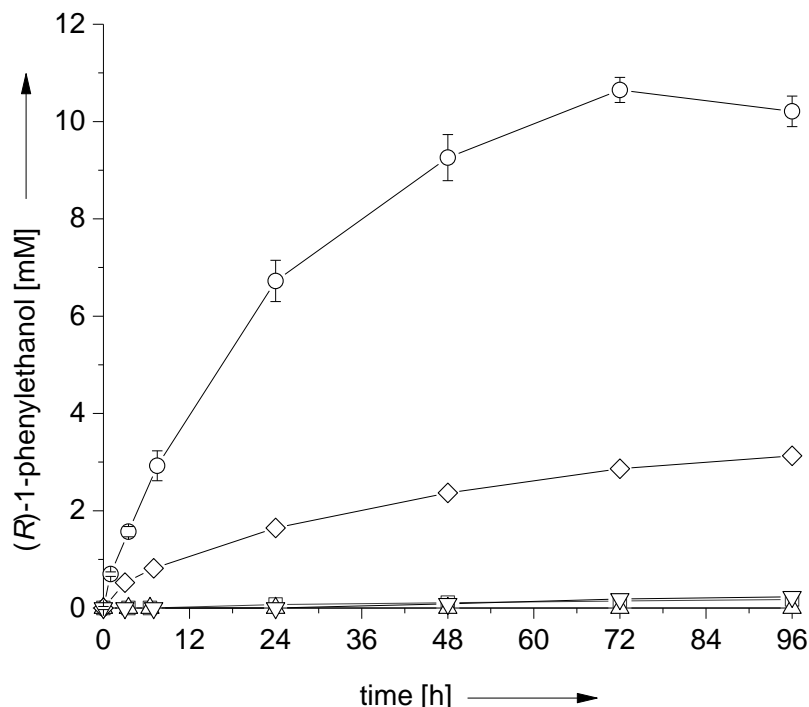


Figure S16. Control experiments to validate the reaction scheme. (○): full cascade as shown in Scheme 1. Control reactions in the absence of enzyme (□), light (△), methanol (◇) or rutile Au-TiO₂ (▽). Reaction conditions: [methanol] = 250 mM, [rutile Au-TiO₂] = 5 g L⁻¹, [rAaeUPO] = 150 nM and [ethylbenzene] = 15 mM in 60 mM phosphate buffer (pH 7.0) under illumination. This supporting Figure is corresponding to Figure 1 in the main text.

Evaporation experiments: effect of exposing the reaction mixture to the ambient atmosphere.

Table S2. Effect of exposure of the reaction system to ambient atmosphere.^[a]

	Bp [°C]	'Open vial' (due to sampling for time course)			Closed vial (no sampling in between)		
		[Substrate] [mM]	[Product] [mM] ^[b]	Evaporation [%] ^[c]	[Substrate] [mM]	[Product] [mM] ^[b]	Evaporation [%] ^[c]
Ethyl benzene	136	0	10.7	22	0.4	12.6	5
Cyclohexane	80.7	0	7.5	45	0.6	11.5	12
Propyl benzene	159	4.8	7.8	7	5.3	7.7	5

^[a] Reaction conditions: [substrate] = 15 mM, [rutile Au-TiO₂] = 5 g L⁻¹, [methanol] = 250 mM and [rAaeUPO] = 150 nM in 60 mM phosphate buffer (pH 7.0) under illumination, t=72 h. ^[b] The corresponding alcohol. ^[c] calculation based on both alcohol and overoxidized ketone.

Influence of the methanol concentration on the photoenzymatic hydroxylation of ethyl benzene.

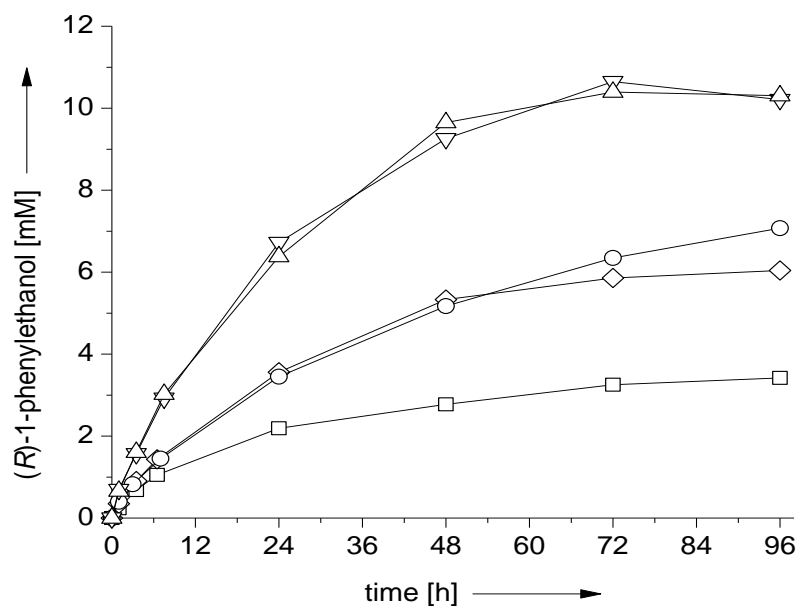


Figure S17. Influence of the methanol concentration on the photoenzymatic hydroxylation of ethyl benzene. Conditions: [methanol] = 250 mM (∇ , 1% v/v), 100 mM (\circ , 0.4 % v/v), 50 mM (\diamond , 0.2 % v/v) and 5 mM (\square , 0.02% v/v), [rutile Au-TiO₂] = 5 g L⁻¹, [rAaeUPO] = 150 nM and [ethylbenzene] = 15 mM in 60 mM phosphate buffer (pH 7.0) under illumination.

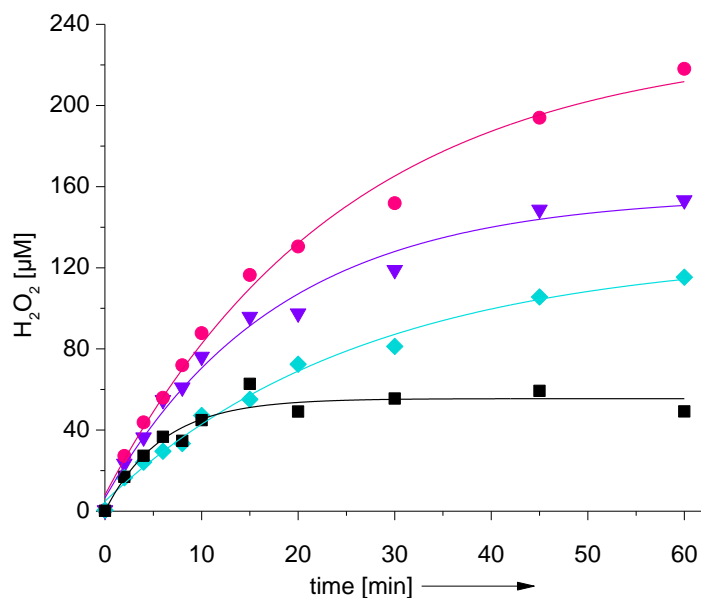
Influence of the methanol concentration on the steady-state H₂O₂ concentration.

Figure S18. Influence of the methanol concentration on the steady-state H₂O₂ concentration. Conditions: [methanol] = 500 mM (\blacktriangle , 2% v/v), 250 mM (\blacktriangledown , 1% v/v), 100 mM (\bullet , 0.4 % v/v), 50 mM (\blacklozenge , 0.2 % v/v), 5 mM (\blacksquare , 0.02% v/v) and [rutile Au-TiO₂] = 5 g L⁻¹ in 60 mM phosphate buffer (pH 7.0) under illumination.

Influence of the photocatalyst concentration on the photoenzymatic hydroxylation of ethyl benzene.

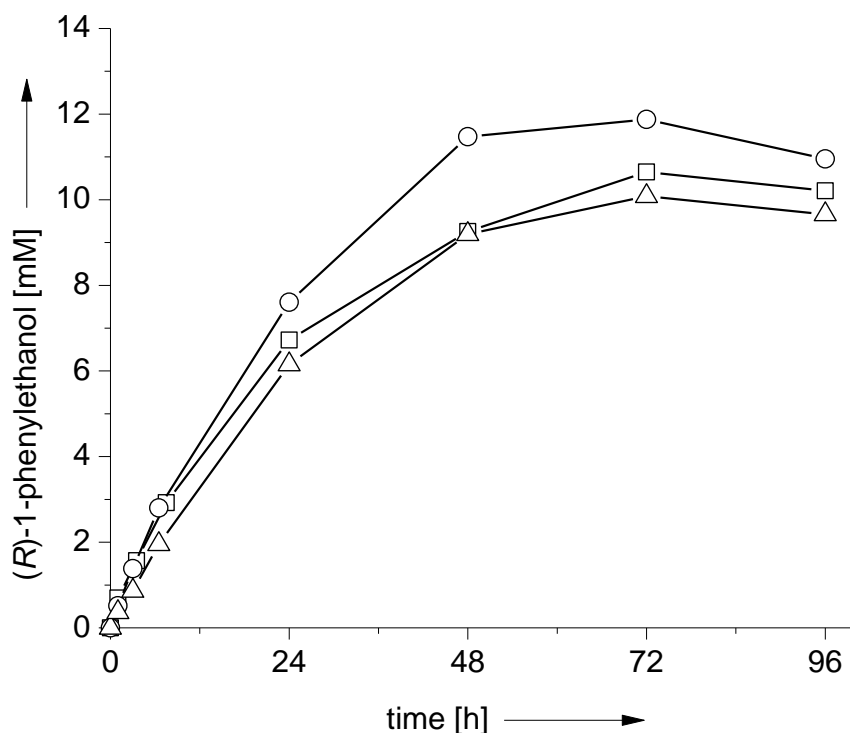


Figure S19. Influence of the photocatalyst concentration on the photoenzymatic hydroxylation of ethyl benzene. Conditions: [rAaeUPO] = 150 nM, [methanol] = 250 mM (1% v/v), [rutile Au-TiO₂] = 5 g L⁻¹ (□), 10 g L⁻¹ (○) and 20 g L⁻¹ (△), and [ethylbenzene] = 15 mM in phosphate buffer (pH 7.0, 60 mM) under illumination.

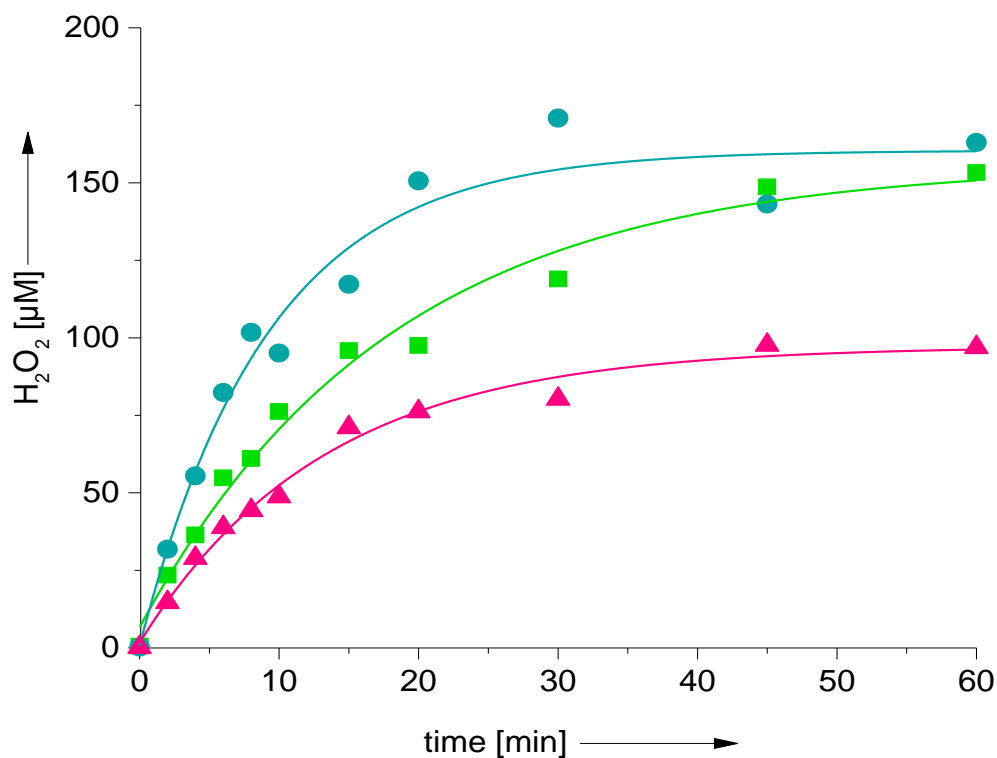
Influence of the photocatalyst concentration on the steady-state H₂O₂ concentration.

Figure S20. Influence of the photocatalyst concentration on the steady-state H₂O₂ concentration. Conditions: [methanol] = 250 mM (1% v/v), [rutile Au-TiO₂] = 5 g L⁻¹ (■), 10 g L⁻¹ (●) and 20 g L⁻¹ (▲) in phosphate buffer (pH 7.0, 60 mM) under illumination.

Influence of the biocatalyst concentration on the photoenzymatic hydroxylation of ethyl benzene.

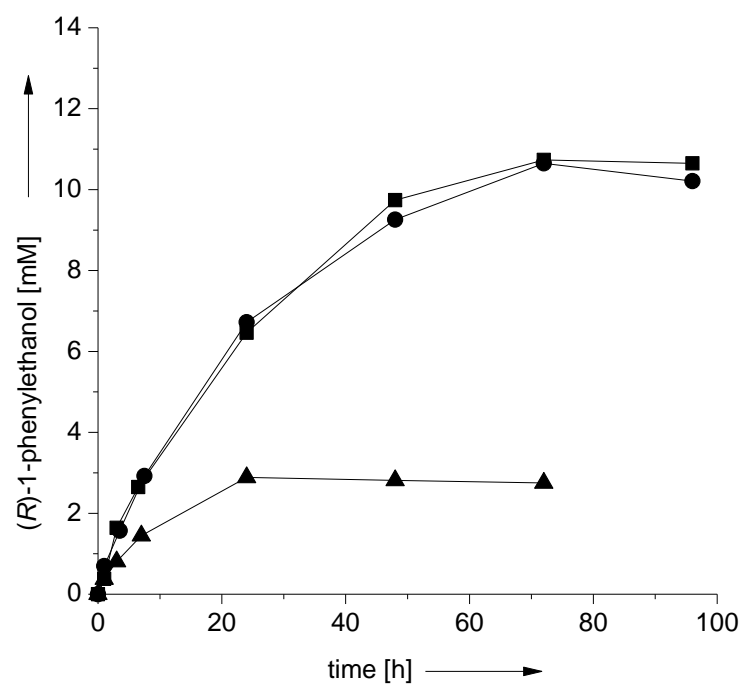


Figure S21. Influence of the biocatalyst concentration on the photoenzymatic hydroxylation of ethyl benzene. Conditions: [rAaeUPO] = 350 nM (■), 150 nM (●) and 50 nM (▲), [methanol] = 250 mM (1% v/v), [rutile Au-TiO₂] = 5 g L⁻¹ and [ethylbenzene] = 15 mM in 60 mM phosphate buffer (pH 7.0) under illumination.

Use of different sacrificial electron donors for the photochemoenzymatic hydroxylation of ethyl benzene.

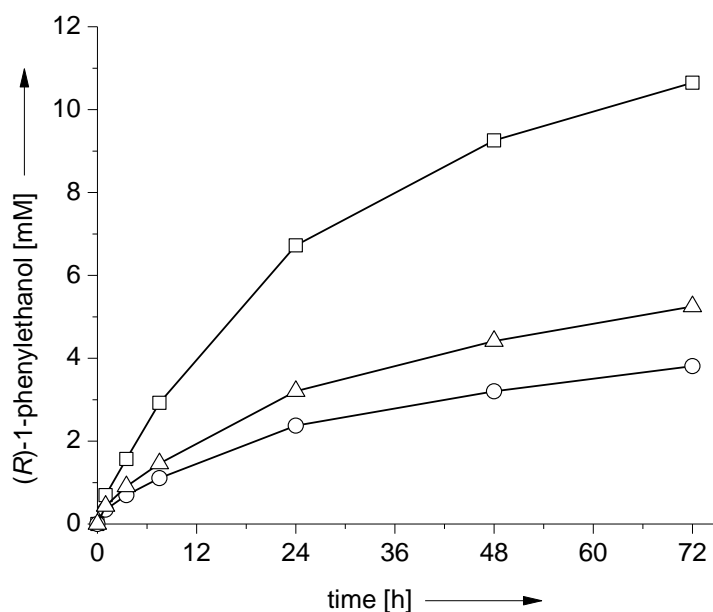


Figure S22. Use of different sacrificial electron donors for the photochemoenzymatic hydroxylation of ethyl benzene. ethanol (O), isopropanol (Δ) and methanol (□). Conditions: [alcohol] = 250 mM (1% v/v), [rAaeUPO] = 150 nM, [rutile Au-TiO₂] = 5 g L⁻¹ and [ethylbenzene] = 15 mM in phosphate buffer (pH 7.0, 60 mM) under illumination.

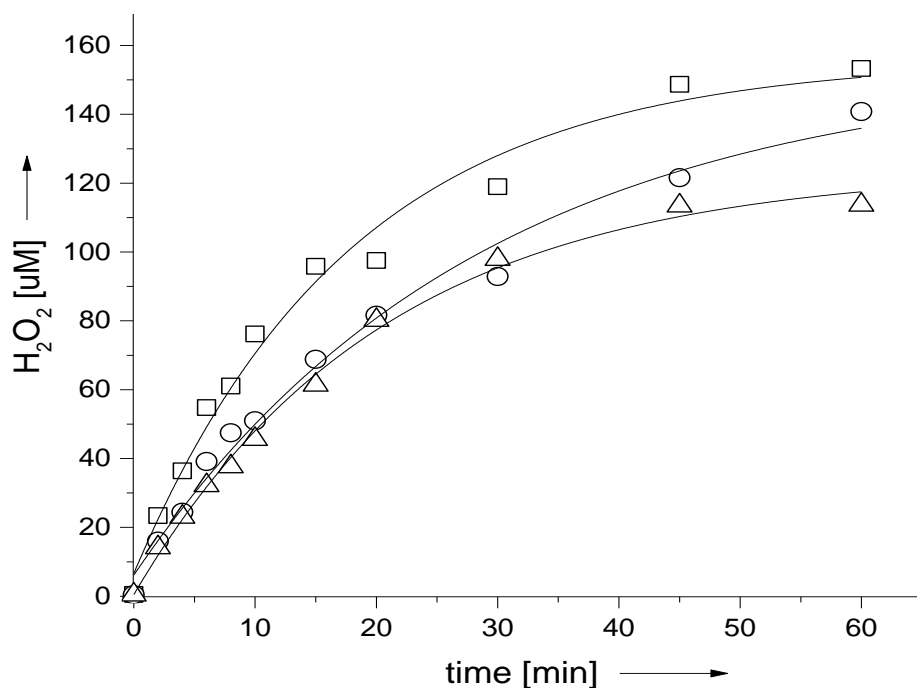
Influence of different sacrificial electron donors on the steady-state H₂O₂ concentration.

Figure S23. Influence of different sacrificial electron donors on the steady-state H₂O₂ concentration. methanol (□), ethanol (O) and isopropanol (Δ). Conditions: [alcohol] = 250 mM (1% v/v), [rutile Au-TiO₂] = 5 g L⁻¹ in phosphate buffer (pH 7.0, 60 mM) under illumination at 30°C.

Influence of formaldehyde or formic acid as sacrificial electron donors on the photochemoenzymatic hydroxylation of ethyl benzene.

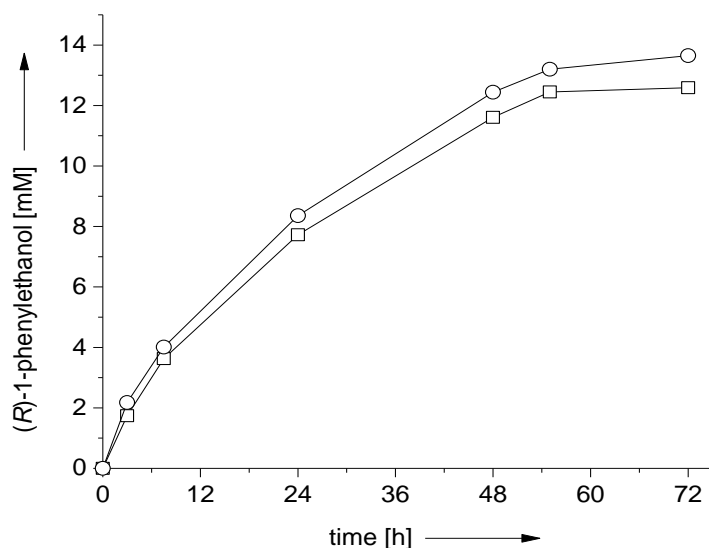


Figure S24. Influence of formaldehyde (○) or formic acid (□) as sacrificial electron donors on the photochemoenzymatic hydroxylation of ethyl benzene. Conditions: [electron donor] = 250 mM; [rAaeUPO] = 150 nM, [rutile Au-TiO₂] = 5 g L⁻¹ and [ethylbenzene] = 15 mM in phosphate buffer (pH 7.0, 60 mM) under illumination.

Influence of formaldehyde or formic acid as sacrificial electron donors on the steady-state H₂O₂ concentration using rutile Au-TiO₂.

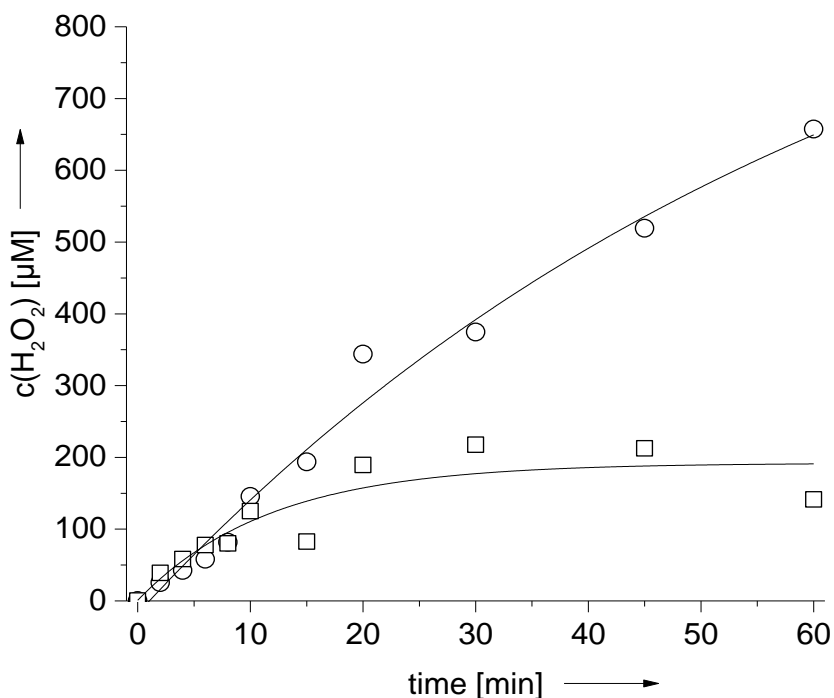


Figure S25. Influence of formaldehyde (○) or formic acid (□) as sacrificial electron donors on the steady-state H₂O₂ concentration using rutile Au-TiO₂. Conditions: [electron donor] = 250 mM; [rutile Au-TiO₂] = 5 g L⁻¹ in phosphate buffer (pH 7.0, 60 mM) under illumination. Reactions using formic acid were performed in phosphate buffer (pH 7.0, 500 mM).

Influence of the photocatalyst loading on the optical transparency of the reaction mixture

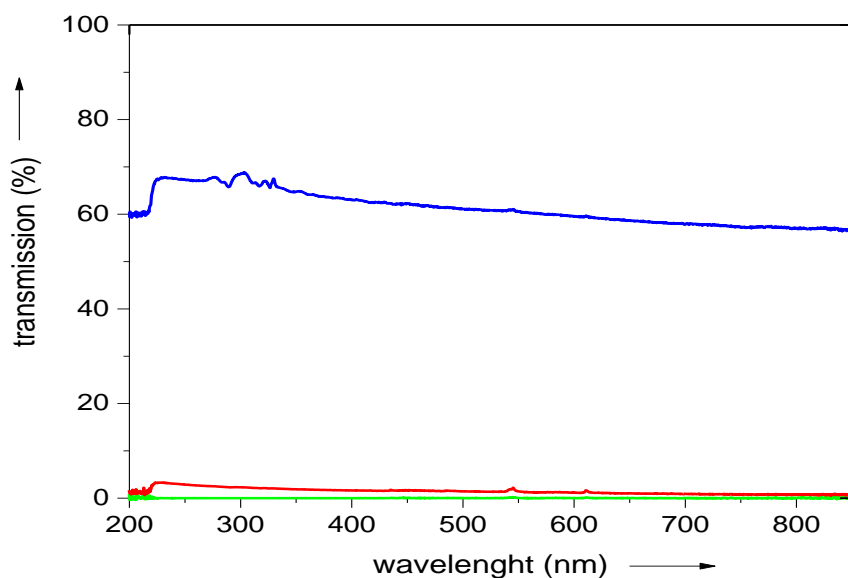


Figure S26. Transmission spectra of Au-TiO₂ suspensions at different concentrations. [Au-TiO₂]: 0.05 g L⁻¹ (blue), 0.5 g L⁻¹ (red) and 5 g L⁻¹ (green); measured in a 1 cm cuvette.

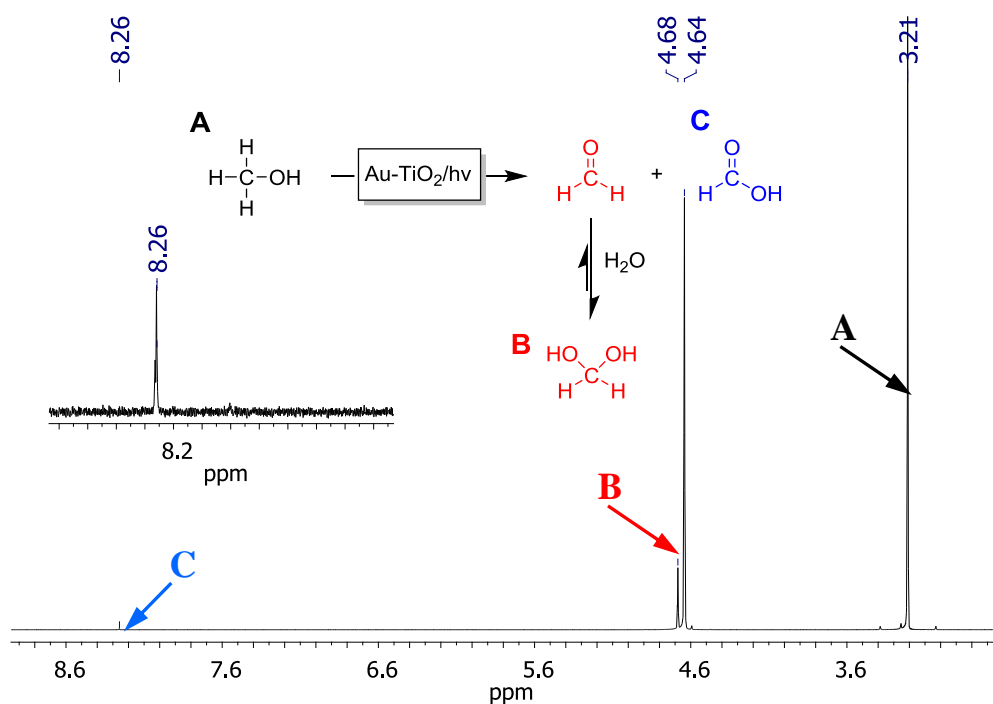
NRM-spectroscopic analysis of the Au-TiO₂-catalysed oxidation of methanol.

Figure S27. ¹H NMR analysis of the photochemical oxidation of methanol. The photooxidation was performed in D₂O for 40 hours using rutile Au-TiO₂ (5 g L⁻¹) and 250 mM of MeOH.

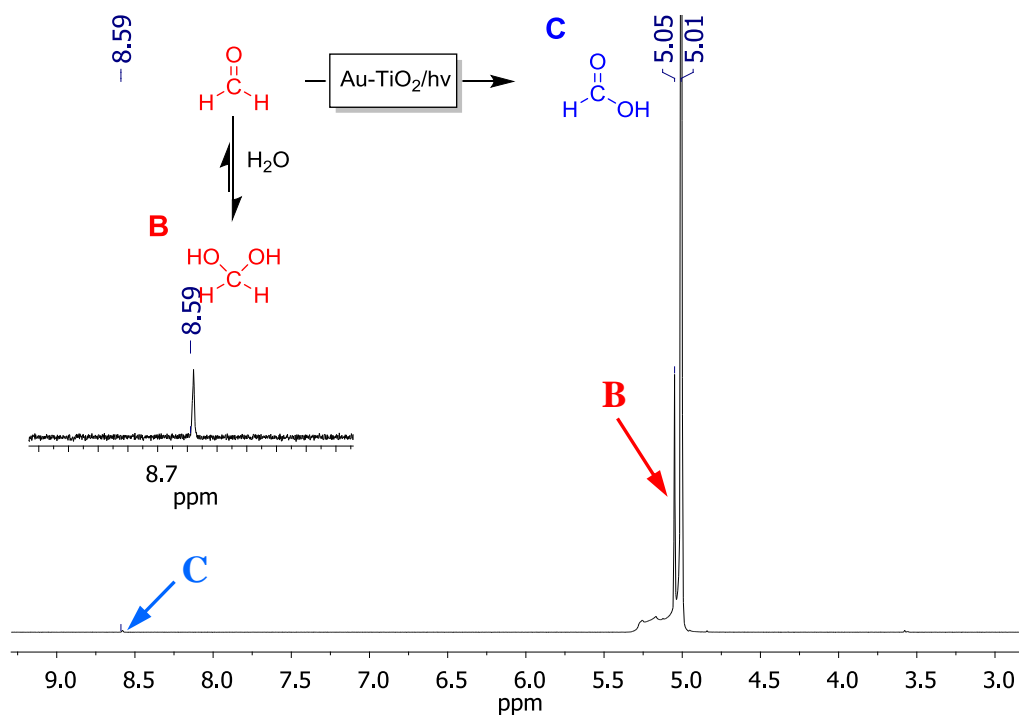
NMR-spectroscopic analysis of the Au-TiO₂-catalysed oxidation of formaldehyde.

Figure S28. ¹H NMR analysis of the photochemical oxidation of formaldehyde. The photooxidation was performed in D₂O for 40 hours using rutile Au-TiO₂ (5 gL⁻¹) and 250 mM of H₂CO.

Comparison of photoenzymatic reactions in the presence and absence of methanol as sacrificial electron donor.

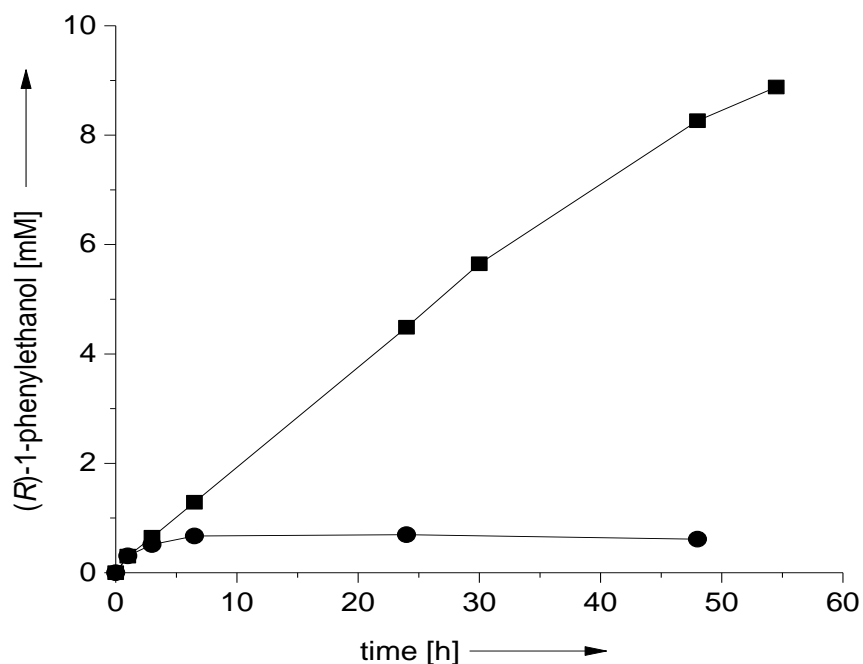


Figure S29. Time courses for the photoenzymatic hydroxylation of ethyl benzene in the presence (■) and absence (●) of MeOH as sacrificial electron donor. Conditions: [methanol] = 250 mM (1% v/v), [anatase Au-TiO₂] = 5 g L⁻¹, [rAaeUPO] = 350 nM and [ethylbenzene] = 15 mM in 60 mM phosphate buffer (pH 7.0) under illumination.

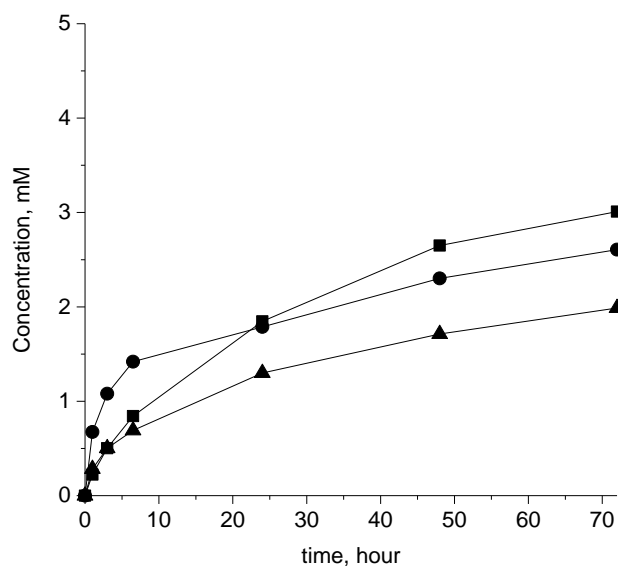


Figure S30. Photoenzymatic hydroxylation reactions of ethyl benzene (■), cyclohexane (●) and propyl benzene (▲) in the absence of sacrificial electron donors such as MeOH. [rutile Au-TiO₂] = 5 g L⁻¹, [rAaeUPO] = 350 nM and [substrate] = 15 mM in 60 mM phosphate buffer (pH 7.0) under illumination.

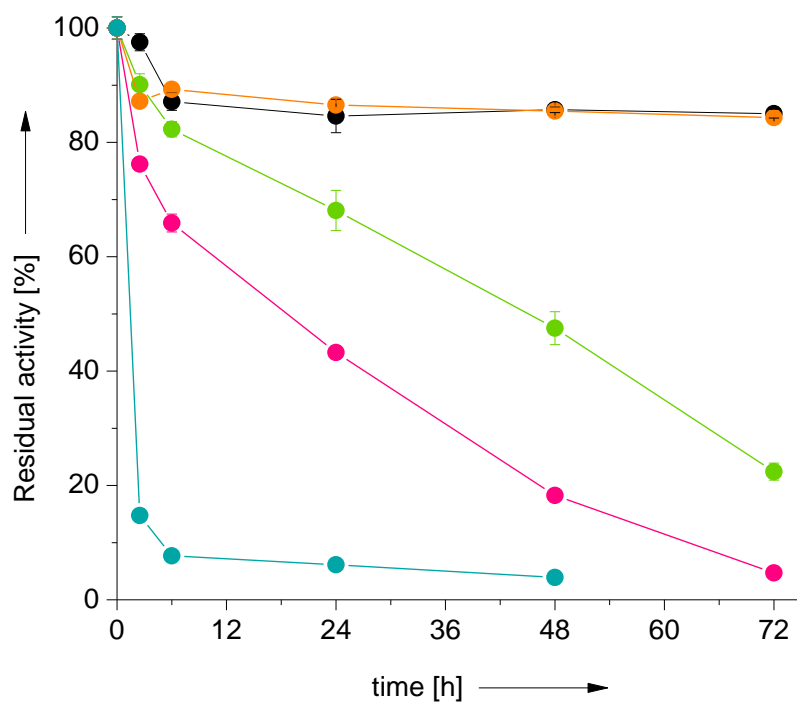
Effect of methanol on the stability of rAaeUPO in the presence of Au-TiO₂.

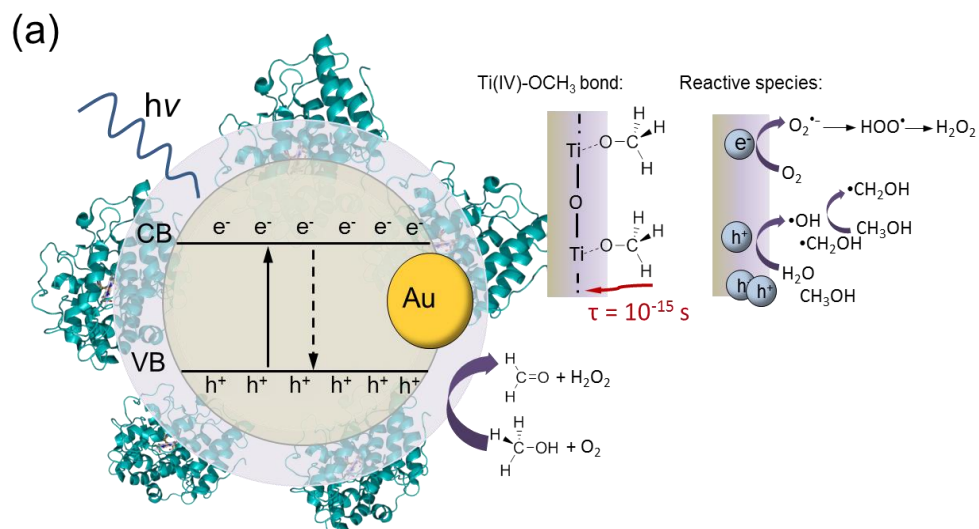
Figure S31. Stability of rAaeUPO under the conditions of the photoenzymatic reaction. Residual rAaeUPO activity after incubation in the presence of the photocatalyst and methanol: MeOH + rAaeUPO in dark (●); MeOH + rAaeUPO under light (●); MeOH + rAaeUPO + rutile Au-TiO₂ in dark (●), rAaeUPO + rutile Au-TiO₂ under light (●) and MeOH + rAaeUPO + rutile Au-TiO₂ under light (●). General conditions: phosphate buffer (60 mM, pH 7.0), T = 30 °C, [rutile Au-TiO₂] = 5 gL⁻¹, [rAaeUPO] = 150 nM and [Methanol] = 250 mM.

Influence of Methanol on the formation rate of hydroxyl radicals

Table S3. Kinetic data of •OH radical formation using rutile Au-TiO₂ in the absence and presence of MeOH as a radical scavenger.

	$k_F(\cdot\text{OH}) / \text{nM min}^{-1}$
no MeOH	409.8
1% MeOH	2.3

Additional information

Elementary steps in Au-TiO₂-catalysed oxidation of water and methanol.

(b)

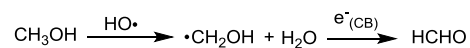
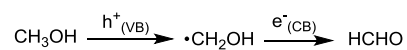
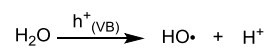
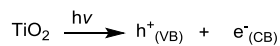


Figure S32. Schematic presentation of methanol oxidation on the surface of Au-TiO₂ surface (a), and two major pathways: hole or $\cdot OH$ -induced methanol oxidation (b).^[9]

Overview over literature-reported hydroxylation reactions and *in situ* H₂O₂ generation systems.

Table S4. Selection of literature examples on the hydroxylation of ethyl benzene.

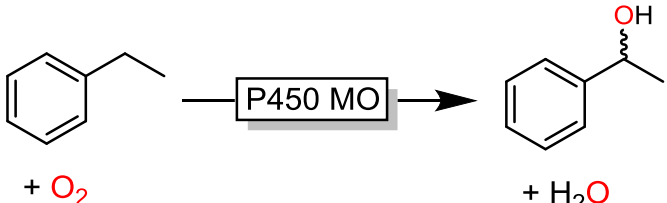
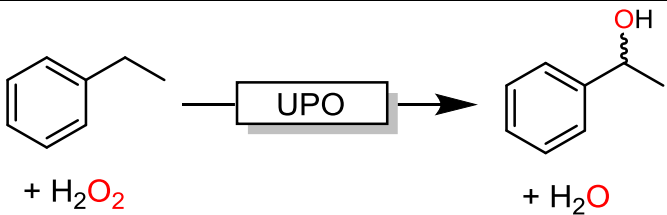
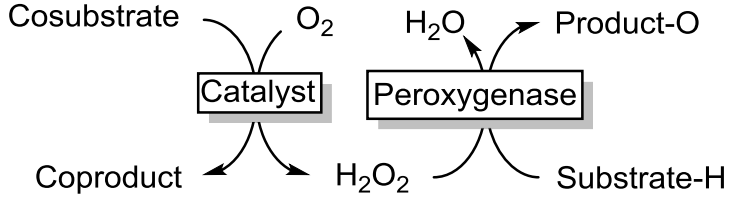
P450 / concentration [μ M]	product [mM]	ee [%]	TON/TOF	Comments	Ref.
					
P450 _{BSβ} from <i>Bacillus subtilis</i> / 1 μ M	0.028	68% (R)	TOF: 28 min ⁻¹	equimolar amounts of H ₂ O ₂ were used instead of NAD(P)H and O ₂	[10]
P450 _{Bm3} from <i>Bacillus megaterium</i> / 0.2 μ M	0.94	62% (R)	TON: 4700		[11]
P450 _{LaMO} CYP116B4 from <i>Labrenzia aggregate</i> / 3 μ M	0.16 mM (18% acetophenone)	99% (S)	TON: 53		[12]
					
CPO / 4.7 μ M	2 mM	97 (R)	TON : 435	peroxygenase using H ₂ O ₂ as oxidant	[13]
rAaeUPO / 100 nM	40 mM	98 (R)	TON: 468 500	4 enzyme cascade for <i>in situ</i> H ₂ O ₂ generation; TONs of the other enzymes were as low as 1300	[14]

Table S5. Overview over some literature known *in situ* H₂O₂ generation methods.

Catalyst	Cosubstrate	Coproduct	waste [g mol ⁻¹ _{product}]	Ref.
				
Glucose oxidase	Glucose	Gluconolactone / Gluconic acid ^[a]	196	[15]
Pd/C	H ₂	-	0	[16]
Cathode	-	-	0	[17]
Alcohol oxidase	Methanol	Formaldehyde	30	[18]
Alcohol oxidase / formaldehyde dismutase / formate dehydrogenase / monooxygenase / NAD	Methanol	CO ₂	14.7	[14]
FMN / hv	EDTA	Ethylene diamine, H ₂ CO, CO ₂	73	[19]

[a] final product due to spontaneous hydrolysis;

Contributions

W. Zhang, B. O. Burek and E. Fernández-Fueyo prepared the catalysts used in this study. These authors also performed the experiments and analysed the results. M. Alcalde, J. Z. Bloh and F. Hollmann conceived the study, analysed the results and prepared the manuscript.

References

- [1] J. B. Priebe, J. Radnik, A. J. J. Lennox, M. M. Pohl, M. Karnahl, D. Hollmann, K. Grabow, U. Bentrup, H. Junge, M. Beller, A. Bruckner, *ACS Catal.* **2015**, *5*, 2137-2148.
- [2] P. Molina-Espeja, E. Garcia-Ruiz, D. Gonzalez-Perez, R. Ullrich, M. Hofrichter, M. Alcalde, *Appl. Environ. Microbiol.* **2014**, *80*, 3496-3507.
- [3] P. Molina-Espeja, S. Ma, D. M. Mate, R. Ludwig, M. Alcalde, *Enz. Microb. Technol.* **2015**, *73-74*, 29-33.
- [4] W. Hemrika, R. Renirie, S. Macedo-Ribeiro, A. Messerschmidt, R. Wever, *J. Biol. Chem.* **1999**, *274*, 23820-23827.
- [5] C. Kormann, D. W. Bahnemann, M. R. Hoffmann, *Environmental Science & Technology* **1988**, *22*, 798-806.
- [6] J. Zhang, Y. Nosaka, *J. Phys. Chem. C* **2013**, *117*, 1383-1391.
- [7] C. G. Hatchard, C. A. Parker, *Proceedings of the Royal Society of London Series a-Mathematical and Physical Sciences* **1956**, *235*, 518-536.
- [8] P. Kubelka, F. Munk, *Zeitschrift für Tech. Phys.* **1931**, *12*, 593-601.
- [9] J. Schneider, M. Matsuoka, M. Takeuchi, J. Zhang, Y. Horiuchi, M. Anpo, D. W. Bahnemann, *Chem. Rev.* **2014**, *114*, 9919-9986.
- [10] O. Shoji, T. Fujishiro, H. Nakajima, M. Kim, S. Nagano, Y. Shiro, Y. Watanabe, *Angew. Chem. Int. Ed.* **2007**, *46*, 3656-3659.
- [11] S. D. Munday, S. Dezvarei, S. G. Bell, *ChemCatChem* **2016**, *8*, 2789-2796.
- [12] Y.-C. Yin, H.-L. Yu, Z.-J. Luan, R.-J. Li, P.-F. Ouyang, J. Liu, J.-H. Xu, *ChemBioChem* **2014**, *15*, 2443-2449.
- [13] A. Zaks, D. R. Dodds, *J. Am. Chem. Soc.* **1995**, *117*, 10419-10424.
- [14] Y. Ni, E. Fernández-Fueyo, A. G. Baraibar, R. Ullrich, M. Hofrichter, H. Yanase, M. Alcalde, W. J. H. van Berkel, F. Hollmann, *Angew. Chem. Int. Ed.* **2016**, *55*, 798-801.
- [15] a) D. Jung, C. Streb, M. Hartmann, *Microporous Mesoporous Mat.* **2008**, *113*, 523-529; b) R. Narayanan, G. Y. Zhu, P. Wang, *J. Biotechnol.* **2007**, *128*, 86-92; c) F. van de Velde, N. D. Lourenço, M. Bakker, F. van Rantwijk, R. A. Sheldon, *Biotechnol. Bioeng.* **2000**, *69*, 286-291.
- [16] S. K. Karmee, C. Roosen, C. Kohlmann, S. Lütz, L. Greiner, W. Leitner, *Green Chem.* **2009**, *11*, 1052 - 1055.
- [17] a) F. Hildebrand, S. Lütz, *Tetrahedron Asymm.* **2007**, *18*, 1187-1193; b) S. Lutz, E. Steckhan, A. Liese, *Electrochem. Commun.* **2004**, *6*, 583-587; c) L. Getrey, T. Krieg, F. Hollmann, J. Schrader, D. Holtmann, *Green Chem.* **2014**, *16*, 1104-1108; d) T. Krieg, S. Huttmann, K.-M. Mangold, J. Schrader, D. Holtmann, *Green Chem.* **2011**, *13*, 2686-2689; e) D. S. Choi, Y. Ni, E. Fernández-Fueyo, M. Lee, F. Hollmann, C. B. Park, *ACS Catal.* **2017**, *7*, 1563-1567.
- [18] a) F. Pezzotti, M. Therisod, *Tetrahedron Asymm.* **2007**, *18*, 701-704; b) F. Pezzotti, K. Okrasa, M. Therisod, *Tetrahedron Asymm.* **2005**, *16*, 2681-2683.
- [19] a) E. Churakova, M. Kluge, R. Ullrich, I. Arends, M. Hofrichter, F. Hollmann, *Angew. Chem. Int. Ed.* **2011**, *50*, 10716-10719; b) D. I. Perez, M. Mifsud Grau, I. W. C. E. Arends, F. Hollmann, *Chem. Comm.* **2009**, 6848 - 6850.